



This discussion paper is/has been under review for the journal Atmospheric Measurement Techniques (AMT). Please refer to the corresponding final paper in AMT if available.

Methodology for determining multilayered temperature inversions

G. J. Fochesatto

Department of Atmospheric Sciences, Geophysical Institute and College of Natural Science and Mathematics, University of Alaska Fairbanks, 903 Koyukuk Dr. Fairbanks, AK, 99775, USA

Received: 6 September 2014 – Accepted: 18 September 2014 – Published: 16 October 2014

Correspondence to: G. J. Fochesatto (foch@gi.alaska.edu)

Published by Copernicus Publications on behalf of the European Geosciences Union.

Methodology for determining multilayered temperature inversions

G. J. Fochesatto

Title Page

Abstract

Introduction

Conclusions

References

Tables

Figures



Back

Close

Full Screen / Esc

Printer-friendly Version

Interactive Discussion



Abstract

The atmospheric boundary layer (ABL) exhibit multilayered thermal structure especially in polar atmosphere during extreme winters. These thermal inversions are originated based on the combined forcing of local and large scale synoptic meteorology. At the local scale the thermal inversion layer forms near the surface and plays a central role in controlling the surface radiative cooling; however, depending upon the large scale synoptic meteorological forcing, an upper level thermal inversion can also exist topping the local ABL.

In this article a numerical methodology is developed to determine all-thermal inversion layers present in a given temperature profile and deduce some of their thermodynamic properties.

The algorithm extract from the temperature profile the most important temperature variations defining thermal layers. This is accomplished by a linear interpolation function of variable length that minimizes an error function. The algorithm functionality is demonstrated on actual radiosonde profiles to deduce all-present inversion layers with an error fraction set independently.

1 Introduction

The atmospheric boundary layer (ABL) is the lowest part of the troposphere in permanent contact with the earth surface and respond to thermal and roughness surface forcing in timescales of minutes to hours (Stull, 1988). Synoptic large scale meteorological processes condition the ABL state by driving relatively rapid horizontal air mass exchange such the case for example of cyclonic air mass advection (Fochesatto et al., 2002) or simply by imposing on upper tropospheric levels an adiabatic compression through the formation of a high pressure anticyclone system (Byers and Starr, 1941; Bowling et al., 1968; Curry, 1983; Cassano et al., 2011). These large scale synoptic processes constraint the temperature of the air mass in tropospheric levels

Methodology for determining multilayered temperature inversions

G. J. Fochesatto

Title Page

Abstract

Introduction

Conclusions

References

Tables

Figures

◀

▶

◀

▶

Back

Close

Full Screen / Esc

Printer-friendly Version

Interactive Discussion



Methodology for determining multilayered temperature inversions

G. J. Fochesatto

Title Page

Abstract

Introduction

Conclusions

References

Tables

Figures

◀

▶

◀

▶

Back

Close

Full Screen / Esc

Printer-friendly Version

Interactive Discussion



without initial connection to the local surface temperature forming vertically localized positive upward thermal gradients called Elevated Inversion (EI) layers (Csanady, 1974; Milionis and Davies, 1992, 2008; Mayfield and Fochesatto, 2013).

Although the ABL-timescale for surface response ranges from minutes to hours (Gar-
rat and Brost, 1981; Stull, 1988); the ABL response to synoptic forcing at local scale
initiated by the radiative and dynamic interaction in the presence of the EIs can vary
from hours to several days depending on a number of factors related to topographic
conditions, temperature and wind distribution, thermal stratification and synoptic air
mass type (e.g., moist cyclone advection or dry anticyclone situations, Mayfield and
Fochesatto, 2013).

In polar atmospheres, the surface energy balance during winter is dominated by
surface radiative exchange (Shulsky and Wendler, 2007). This exchange occurs be-
tween a shallow layer close to the ground capped by the surface based inversion (SBI)
top height. The SBI also plays a thermalizing role in the surface cooling process by
promoting radiative equilibrium between surface long-wave emission and the air mass
radiative emission contained within the SBI layer depth (Malingowski et al., 2014). The
SBI is present normally under non-advective conditions over ice and snow covered
surfaces and is a common feature in continental places as well as in Arctic oceanic
and maritime environments (Overland and Guest, 1991; Bintanja et al., 2011). The
SBI formation and persistence is also strongly dependent on terrain morphology and
orientation (e.g., formation of cold pools Mahrt et al., 2001; Clements et al., 2003;
Whiteman and Zhong, 2008; Fochesatto et al., 2013). Of particular interest is the for-
mation and breakup of the SBI layer (Billelo, 1966; Hartman and Wendler, 2005) and
it's thermal regime across time as it forms (i.e., fast cooling at the formation process
followed by a growing depth phase) (Malingowski et al., 2014). In such cases what is
important is not only to be able to determine the inversion top height and its thermal
strength (or gradient) but also the existence of stratified levels (positive dT/dz) close to
the surface which are thermodynamic features controlling the sensible and latent heat
exchange rate (Raddatz et al., 2011a, b). In addition simultaneous determination and

Methodology for determining multilayered temperature inversions

G. J. Fochesatto

Title Page

Abstract

Introduction

Conclusions

References

Tables

Figures

◀

▶

◀

▶

Back

Close

Full Screen / Esc

Printer-friendly Version

Interactive Discussion



characterization of EI layers and SBI has the potential to improve assessment on local air pollution meteorology (Andre and Mahrt, 2005), improve forecasting of freezing rain episodes (Robbins and Cortinas, 2002), determine heat exchanges in unconsolidated sea-ice surfaces (Raddatz et al., 2013a, b) and potential impact on Arctic climate (Bintanja et al., 2011).

The most widely used instrumentation to observe the ABL is in-situ temperature determination by high resolution radiosondes. However the methodologies to analyze the radiosonde temperature profile, see for example (Seidel et al., 2010), still do not account for complex embedded thermal structures of several types. Such an example are winter high latitude temperature profiles in which the occurrence of combined stratified, isothermal layers and inversion layers are normally found close to the ground. On the other hand some authors have classified these layers as being short-living structures and therefore discarded from their analysis (Kahl, 1990; Serreze et al., 1992). However, it was recently demonstrated during the Winter Boundary-Layer Experiment (Wi-BLE_x) (Fochesatto et al., 2013; Mayfield and Fochesatto, 2013; Malinowski et al., 2014) that all mentioned thermal structures persist with some changes through the day depending on environmental conditions.

Nonetheless, trying to detail more in-depth turbulent mixing processes in the ABL, the observations demands instrumentation that can profile the atmosphere at higher spatial and temporal resolution than what provides a radiosonde instrument. Thus active remote sensing instruments gives a better description of the vertical structure and dynamics of the ABL by means of for example Lidar (Light Detection And Ranging, Fochesatto et al., 2001a, b; Fochesatto et al., 2004) and sodar (SOund Detection And Ranging, Beyrich and Weill, 1993; Fochesatto et al., 2013). Particularly interesting is the high temporal and spatial resolution at which lidars can describe the initiation of convection close to the surface as well as simultaneously describe the dynamics of EI layers in this case also known as residual layer (Fochesatto et al., 2001a, b). Similarly, insightful description of the turbulent and dynamic structure of the ABL when shallow cold flows penetrate the stable ABL can be gained by using a sodar profilers

Methodology for determining multilayered temperature inversions

G. J. Fochesatto

Title Page

Abstract

Introduction

Conclusions

References

Tables

Figures

◀

▶

◀

▶

Back

Close

Full Screen / Esc

Printer-friendly Version

Interactive Discussion



(Fochesatto et al., 2013). Passive ground based remote sensors i.e., microwave radiometers, based on background sky microwave radiation sensing are another option to profile the ABL at \sim minute resolution (Cadeddu et al., 2002). Methodologies to determine the ABL height using lidars are based on detecting the changes in the optical backscattering top inversion level when the laser beam crosses the interface between the air mass in the ABL and the free troposphere (Menut et al., 1999; Bianco and Wilczak, 2002; Brooks, 2003; Lammert and Bosenberg, 2006). On the other hand determining the ABL height using sodar becomes a little more complicated because the observations give access to the temperature structure of turbulence C_T^2 profile that changes depending upon the ABL phase, terrain and multilayer structured (Beyrich and Weill, 1993).

Radiosonde determination of thermal inversion layers to study the Arctic Ocean ABL has been done using function fitting on radiosonde in the Arctic Ocean (Serreze et al., 1992). To determine the large scale climate signature in the SBI time-series of polar regions Arctic and Antarctic (Seidel et al., 2010; Zhang and Seidel, 2011; Zhang et al., 2011). In short term studies, Khal (1990) and Khal et al. (1992) have implemented a methodology to explore the temperature profile and then applying some constraints deduce the SBI top height. And, using similar methodologies trying to link time-series of SBI top heights to large scale climate processes in continental Alaska (Bourne et al., 2010).

In this article a mathematical procedure is described and its numerical implementation is documented to determine all-thermal layers presents on a given temperature profile in the lower troposphere. Section 2 describes the mathematical procedure and numerical implementation, Sect. 3 determine the calibration factors of the numerical methodology, Sect. 4 applies the numerical procedure to routinely radiosonde observations and Sect. 5 gives a final assessment of the implemented numerical methodology.

2 Methodology

A thermal inversion represents a region in the atmosphere defining a positive upward temperature gradient $\frac{dT}{dz} > 0$, where, T is the temperature and z is the height. As described in the introduction this positive upward temperature gradient can have two origins. The first one related to surface cooling i.e., surface net radiation loss, giving origin to the formation of a SBI and, the second one is originated after synoptic large scale processes i.e., upper level warming also known as EI layers (Mayfield and Fochesatto, 2013). Under these conditions the temperature profile in the lower troposphere is expected to describe either a neutral thermal layer (no inversion present), isothermal layers, presence of a surface based-inversion (SBI), development of stratified layers within the SBI layer-depth, shallow inversion layers above the SBI-inversion top and more complex situations in which upper level thermal inversions are also present with base and top in the outflow ABL (Khal, 1990; Mayfield and Fochesatto, 2013). Figure 1 sketches the more relevant situations.

To deduce the total existing thermal layers composing the temperature profile a computational routine was implemented to identify the heights and temperatures of the base and top of stratified and inversion layers. In this case the temperature profile was reduced to a mathematical expression based on a linear function calculated on the basis of an iterative linear interpolation routine. The numerical routine is based on fitting and refitting a piecewise linear interpolating function with variable length to define layer-by-layer the temperature profile composition. An error quote controls the algorithm convergence and is calculated based on the largest singular value ε by which all thermal features in the temperature profile can be reproduced based on an error difference preset in the routine. The numerical method actually reduces the number of points presents in the original temperature profile. Therefore after applying the numerical methodology the temperature profile now becomes a data structure defining thermodynamic characteristics of thermal layers found in the temperature profile. Further on, exploring the data structure we can define essential features in the temperature

Methodology for determining multilayered temperature inversions

G. J. Fochesatto

Title Page

Abstract

Introduction

Conclusions

References

Tables

Figures

◀

▶

◀

▶

Back

Close

Full Screen / Esc

Printer-friendly Version

Interactive Discussion



Eq. (3):

$$\phi(z) = \sum_{k=1}^{k=p} m_k \cdot z + b_k \quad (3)$$

where p is the total number of points from the original temperature profile that has been retained by the fitting process.

Table 1 indicates a five-layer temperature structure in the ABL up to 1 km height based on six-point temperature simulation. The profile defines a stratified SBI with top height at 250 m topped by an EI at 670 m. Figure 2 illustrate the sequences in which the algorithm operates to search and define each layer from 1 to 5. In this case we retain all points in the temperature profile.

3 Convergence error

Since the ability of the algorithm to extract thermal layers depends upon the value chosen for ε then it is reasonable to determine for example how that value changes as function of temperature profile gradient dT/dz to be retrieved represented by an amount of ($^{\circ}\text{C}/100\text{ m}$) as the minimum temperature gradient threshold. To deduce the calibration curve of ε as function of the thermal gradient threshold a simulation was performed scanning values of ε from 0.1 to 10 as function of desired thermal gradients thresholds from 0.1 to $15^{\circ}\text{C}/100\text{ m}$ (Mayfeild and Fochesatto, 2013) . Once a threshold dT/dz is defined a maximum convergence value ε can be selected to actually detect the prescribed thermal layer.

Figure 3 illustrate the calibration curve of the thermal gradient threshold as function of the preset error value ε . This relationship can of course be determine in an ideal scenario since a real temperature profile will manifest a diverse structure in which the error will be dependent on the multiple thermal features present in the profile. Therefore in this case a constant temperature vertical profile was assumed with a thermal gradient

Methodology for determining multilayered temperature inversions

G. J. Fochesatto

Title Page

Abstract

Introduction

Conclusions

References

Tables

Figures

◀

▶

◀

▶

Back

Close

Full Screen / Esc

Printer-friendly Version

Interactive Discussion



Methodology for determining multilayered temperature inversions

G. J. Fochesatto

Title Page

Abstract

Introduction

Conclusions

References

Tables

Figures

◀

▶

◀

▶

Back

Close

Full Screen / Esc

Printer-friendly Version

Interactive Discussion



that was set at one prescribed height with variable thermal strength in ($^{\circ}\text{C}/100\text{ m}$). The strength of this thermal gradient was varied by intervals from 0.1 to 1.0 in steps of 0.1 then, from 1.0 to 10 in steps of 1.0 and for ε values from 0.1 to 10 in steps of 0.1. Thus the ability to find the thermal gradient was deduced at each thermal gradient level as a function of ε and a number 1 to 4 of thermal layers present simultaneously. The value found for ε ensures detection of the proposed thermal gradient and all-those larger presents simultaneously in the temperature profile.

As an example let's imagine we would like to detect thermal layers in a temperature profile with a threshold of $4^{\circ}\text{C}/100\text{ m}$ then according to Fig. 3 the preset ε should be 3.9 or less to ensure detection of the single thermal layer. But ε relaxes as the number of calculated thermal layers present in the profile increases. For example ε can be less than 5.0 if two layers with the same gradient are present and less than 6.9 if three layers are present and less than 7.9 if four layers or more are present. On the other hand, as the thermal gradient threshold decreases the values of ε needed are smaller. Conversely, if the thermal gradient relaxes then ε is also seen to relax. From Fig. 3 from this analysis it can be concluded that practically all thermal layers are detected after $10^{\circ}\text{C}/100\text{ m}$ with $\varepsilon = 10$ or less. However it can be seen that single layer detection imposes the more restricted condition in terms of ε . For example if the desired thermal gradient threshold is $7^{\circ}\text{C}/100\text{ m}$ and the ε is set to values larger than 7.5; then a temperature profile having a single layer present will not be detected while instead if the temperature profile is composed by two and more layers then that ε value will be enough.

4 Numerical application

In this section the numerical method is applied to the restitution of thermal layers from radiosonde data. In this case we used radiosonde data archives from the NOAA-ESRL database for the Fairbanks International Airport WMO station code 70261. The case of 15 January 2014 at 00:00 UTC is examined here to illustrate the numerical

methodology. Figure 4 illustrates the temperature profile below 5 km, above ground level. Table 2 summarizes all layer's information extracted presetting $\varepsilon = 0.1$ allowing detecting 24 layers over 42 temperature points below 5 km.

From the analysis of detected layers one can initially search in the data structure the changes in m_k . Since $m_k > 0$ will be assigned to positive upward dT/dz while negative will indicate the opposite. The third case $m_k \sim 0$ will be the case not very often found but retrieved when sufficient resolution is present indicating isothermal layers. From the analysis of the resulted data it can be deduced that the inversion layer defined when m_k changes from positive to negative, is assigned to be the SBI at 165 m a.g.l.; while on the other hand any other inversion layer with base off the ground is called therefore EI. In this particular case the methodology found two EI's with base heights at 685 m and 1108 m a.g.l. A stratified layer was detected by the algorithm at 62 m ($5.2^\circ\text{C}/100\text{m}$) within the SBI layer depth and similarly other stratified layers are present between the SBI top height and the EI layers as indicated in Table 2.

Furthermore, the algorithm performance was evaluated using the present case example in term of the number of layers detected as function of the preset convergence error ε and the final temperature retrieved error (%) as function of the preset ε value. In this case the algorithm was executed in a loop varying ε in the interval from 0.1 to 1.0 in steps of 0.1 and from 1.0 to 15 in step of 0.5. The final temperature error was computed based on the *norm* of the final temperature vector resampled in terms of the original height vector. This explain why the actual preset ε value which applies to every step in the fitting and re-fitting process is somewhat different to the final temperature profile error after fitting all the thermal layers. Figure 5 depicts two curves indicating the number of thermal layers retrieved and the final overall temperature error profile as function of the ε preset value.

In order to summarize the application of this methodology and visualize the effects of the final error over the reconstructed temperature profile; Fig. 6 illustrate the resampled temperature profile in the case of four selected error levels.

Methodology for determining multilayered temperature inversions

G. J. Fochesatto

Title Page

Abstract

Introduction

Conclusions

References

Tables

Figures

◀

▶

◀

▶

Back

Close

Full Screen / Esc

Printer-friendly Version

Interactive Discussion



Methodology for determining multilayered temperature inversions

G. J. Fochesatto

Title Page

Abstract

Introduction

Conclusions

References

Tables

Figures

◀

▶

◀

▶

Back

Close

Full Screen / Esc

Printer-friendly Version

Interactive Discussion



It is clear that error = 0.1 % reproduces all layers shown in the original temperature profile while by increasing the preset convergence factor $\epsilon = 0.1, 1.0, 5.5, 10.5$ the error in the overall temperature retrieved profile increases and therefore the fine structure in the temperature profile vanishes. This is very important to consider. For example, for more than 10 % of error the entire ABL thermal structure disappears indicating just the presence of the EI-1 below 1500 m.

5 Summary

A simple numerical iterative routine was developed to deduce all thermal layers composing a given atmospheric temperature profile. The numerical routine converts the temperature profile in a reduced data structure containing base and top heights as well as thermal gradients allowing identification of most important air mass changes accounting for SBI, SL, EI and isothermals layers.

This methodology has been applied to the study of 10 years. upper air data in the interior of Alaska and to deduce the statistical significance of the presence of SBI and multilevel EIs. In addition, the application of this methodology allowed classification of EI layers by means of the dew point temperature gradient across the inversion layer depth (Mayfield and Fochesatto, 2013).

The method was also applied to study the temporal evolution of SBIs using high resolution GPS soundings during formation and breakup of SBI layers (Malingowski et al., 2014).

The method does not introduce new temperature points it rather reduces the amount of them according to the preset convergence value. However some degree of expertise in meteorology is needed to read the output data-structure and classify the detected thermal layers.

Based on this methodology temporal series of inversion heights can be formed analyzing the data output structure and after applying a specific criteria extract a time series of a particular nature. For example, in Mayfield and Fochesatto (2013), the interest

Methodology for determining multilayered temperature inversions

G. J. Fochesatto

Title Page

Abstract

Introduction

Conclusions

References

Tables

Figures

◀

▶

◀

▶

Back

Close

Full Screen / Esc

Printer-friendly Version

Interactive Discussion



was to perform a statistical analysis of SBI and EI-1 to -4 layers and classify them in terms of their dew point temperature gradient across the inversion. For that purpose, it was necessary to include the dew point temperature in the data-structure after reading and processing the radiosonde data so that the retrieved EI layer could have been classified.

The relationship between threshold thermal gradient dT/dz , the preset convergence factor ε and the overall final error between the resampled temperature profile and the original temperature profile is difficult to establish. Section 3 deals with the relationship between dT/dz and ε for theoretical profiles (i.e., constant temperature profile with controlled thermal inversions) to deduce this relationship. However the application of this methodology to a real case produces an overall error in the resampled profile that is different from the prescribed preset convergence factor ε . This is important to differentiate since ε applies internally as convergence factor to increase fidelity in the temperature fitting over an Euclidean norm that is applied over a variable vector length step by step. While, on the other hand, the overall error indicating how accurate the resampled temperature profile reproduces the original profile accounts for the entire profile at once.

The application of such methodology has numerous venues. For instance air pollution meteorology and pollutants transport processes that are strongly dependent of meteorological conditions nearby the emission source. In special at high latitudes where the SBI layers and stratified-SBI shows a persistent presence during the winter in the absence or under little diurnal cycle. The application of this methodology is not restricted to low level layers exclusively since it has been demonstrated by Mayfield and Fochesatto (2013) that EI layers also plays an important role in the high latitude ABL because of the dynamic radiative forcing that drives surface warming and pollutants recirculation. Another application is the evaluation of large scale synoptic meteorological changes and its impact on high latitude environment. In this case it is important to consider a methodology that can account for all thermal layers present in the temperature profile over ocean, maritime and continental places. In order to be able to evaluate the

Methodology for determining multilayered temperature inversions

G. J. Fochesatto

Title Page

Abstract

Introduction

Conclusions

References

Tables

Figures

◀

▶

◀

▶

Back

Close

Full Screen / Esc

Printer-friendly Version

Interactive Discussion



impact of prescribed synoptic meteorological patterns over a specific area it is necessary to retrieve simultaneously thermal layers affected by local scale and those dominated by large scale atmospheric motion. Therefore evaluation of temporal series containing this multilayered information could assist in improving our understanding of how large scales feedbacks are introduced and affect the local environment. Since radiative interaction between SBI and EI layers is controlled by the vertical stratification then the analysis of surface warming in high latitude continental and oceanic environments in particular over sea-ice surfaces will be one future application of this methodology. Of course data bases in which the method can be applied need to have sufficient vertical resolution to pull level details close to the surface to be able to define the multilayered structure.

The retrieval of stratified layers may results perhaps of no practical importance for operational meteorological purposes but it is of course of importance in determination of heating rates in studying the effect of inversion layers in surface–atmosphere interaction either on continental and in sea-ice surfaces. In terms of transient air pollution process, the importance of stratified layers within the SBI, is on of the most important limiting factor for turbulent diffusion for example during rush hours where high concentration of particulate matter and noxious gases build up to dangerous levels in short period of time.

The algorithm was proposed for radiosonde profiles but it can also process temperature outputs from microwave radiometers and large scale reanalysis databases as well as climate outputs downscaled temperature profiles. Particularly interesting is the use of this algorithm to climatological determination of the ABL layers SBI and EI and their connection to large scale synoptic meteorology.

Acknowledgement. This research was funded by the Division of Air Quality from the Department of Environmental Conservation of Alaska and the Air Quality Office of the Fairbanks North Star Borough (funding number G00006433-398755). The author was supported by the Geophysical Institute, University of Alaska Fairbanks. The author acknowledge the use of the NOAA/ESRL reanalysis database.

References

- André, J. C. and Mahrt, L.: The nocturnal surface inversion and influence of clear-air radiative cooling, *J. Atmos. Sci.*, 39, 864–878, 1982.
- Beyrich, F. and Weill, A.: Some aspects of determining the stable boundary-layer depth from sodar data, *Bound.-Layer Meteorol.*, 63, 97–116, 1993.
- 5 Bianco, L. and Wilczak, J.: Convective boundary layer depth: improved measurement by Doppler Radar wind profiler using fuzzy logic methods, *J. Atmos. Ocean Tech.*, 19, 1745–1758, 2002.
- Billelo, M. A.: Survey of arctic and subarctic temperature inversions. US Army Cold Regions Research & Engineering Laboratory, Hanover NH, pp: 36. TR 161, 1966.
- 10 Bintanja, R., Graversen, R. G., and Hazeleger, W.: Arctic winter warming amplified by the thermal inversion and consequent long infrared cooling to space, *Nat. Geosci.*, 4, 758–761, doi:10.1038/ngeo1285, 2011.
- Bourne, S. M., Bhatt, U. S., Zhang, J., and Thoman, R.: Surface-based temperature inversions in Alaska from a climate perspective, *Atmos. Res.*, 95, 353–366, 2010.
- 15 Bowling, S. A., Ohtake, T., and Benson, C. S.: Winter pressure systems and ice fog in Fairbanks, Alaska, *J. Appl. Meteorol.*, 7, 961–968, 1968.
- Bradley, R. S., Keimig, F. T., and Diaz, H. F.: Climatology of surface-based inversions in the North American Arctic, *J. Geophys. Res.*, 97, 15699–15712, 1992.
- 20 Brooks, I. M.: Finding boundary layer top: application of a wavelet covariance transform to lidar backscatter profiles, *J. Atmos. Ocean. Tech.*, 20, 1092–1105, 2003.
- Byers, H. R. and Starr, V. P.: The circulation of the atmosphere in high latitudes during winter, *Mon. Weather Rev. Suppl. No. 47*, 34, 1941.
- Cadeddu, M. P., Peckham, G. E., and Gaffard, C.: The vertical resolution of ground-based microwave radiometers analyzed through a multiresolution wavelet technique, *Geosci. Remote Sens.*, 40, 531–540, doi:10.1109/TGRS.2002.1000313, 2002.
- 25 Cassano, E. N., Cassano, J. J., and Nolan, M.: Synoptic weather pattern controls on temperature in Alaska, *J. Geophys. Res.*, 116, D11108, doi:10.1029/2010JD015341, 2011.
- Clements, C., Whiteman, C., and Horel, J.: Cold-air-pool structure and evolution in a mountain basin: Peter Sinks, Utah, *J. Appl. Meteorol.*, 42, 752–768, 2003.
- 30 Csanady, G. T.: Equilibrium theory of the planetary boundary layer with an inversion lid, *Bound.-Layer Meteorol.*, 6, 63–79, 1974.

Methodology for determining multilayered temperature inversions

G. J. Fochesatto

Title Page

Abstract

Introduction

Conclusions

References

Tables

Figures

◀

▶

◀

▶

Back

Close

Full Screen / Esc

Printer-friendly Version

Interactive Discussion



Methodology for determining multilayered temperature inversions

G. J. Fochesatto

Title Page

Abstract

Introduction

Conclusions

References

Tables

Figures

◀

▶

◀

▶

Back

Close

Full Screen / Esc

Printer-friendly Version

Interactive Discussion

- Holmgren, B., Spears, L., Wilson, C., and Benson, C.: Acoustic soundings of the Fairbanks temperature inversions, in: *Climate of the Arctic*, edited by: Weller, G. and Bowling, S. A., Proceedings of the AAAS-AMS conference, Fairbanks, Alaska, 293–306, 1975.
- Huff, D. M., Joyce, P. L., Fochesatto, G. J., and Simpson, W. R.: Deposition of dinitrogen pentoxide, N_2O_5 , to the snowpack at high latitudes, *Atmos. Chem. Phys.*, 11, 4929–4938, doi:10.5194/acp-11-4929-2011, 2011.
- Kahl, J.: Characteristics of the low-level temperature inversion along the Alaskan Arctic coast, *Int. J. Climate*, 10, 537–548, 1990.
- Kahl, J. D., Serreze, M. C., and Schnell, R. C.: Tropospheric low-level temperature inversions in the Canadian Arctic, *Atmos. Ocean*, 30, 511–529, 1992.
- Lammert, A. and Bosenberg, J.: Determination of the convective boundary-layer height with laser remote sensing, *Bound.-Layer Meteorol.*, 119, 159–170, 2006.
- Mahrt, L., Vickers, D., Nakamura, R., Sun, J., Burns, S., and Lenschow, D.: Shallow drainage flows, *Bound.-Layer Meteorol.*, 101, 243–260, 2001.
- Malingowski, J., Atkinson, D., Fochesatto, G. J., Cherry, J., and Stevens, E.: An observational study of radiation temperature inversions in Fairbanks, Alaska, *Polar Sci.*, 8, 24–39, 2014.
- Mayfield, J. A. and Fochesatto, G. J.: The layered structure of the winter atmospheric boundary layer in the interior of Alaska, *J. Appl. Meteorol. Clim.*, 52, 953–973, 2013.
- Menut, L., Flamant, C., Pelon, J., and Flamant, P. H.: Urban boundary-layer height determination from lidar measurements over the Paris area, *Appl. Optics*, 36, 945–954, 1999.
- Milionis, A. E. and Davies, T. D.: A five-year climatology of elevated inversions at Hemsby (UK), *Int. J. Climatol.*, 12, 205–215, 1992.
- Milionis, A. E. and Davies, T. D.: The effect of the prevailing weather on the statistics of atmospheric temperature inversions, *Int. J. Climatol.*, 28, 1385–1397, 2008.
- Overland, J. E. and Guest, P. S.: The Arctic snow and air temperature budget over sea ice during winter, *J. Geophys. Res.*, 96, 4651–4662, 1991.
- Raddatz, R. L., Galley, R. J., Candlish, L. M., Asplin, M. G., and Barber, D. G.: Integral profile estimates of sensible heat flux from an unconsolidated sea-ice surface, *Atmos. Ocean*, 51, 135–144, doi:10.1080/07055900.2012.759900, 2013a.
- Raddatz, R. L., Galley, R. J., Candlish, L. M., Asplin, M. G., and Barber, D. G.: Integral profile estimates of latent heat flux under clear skies at an unconsolidated sea-ice surface, *Atmos. Ocean*, 51, 239–248, doi:10.1080/07055900.2013.785383, 2013b.

Methodology for determining multilayered temperature inversions

G. J. Fochesatto

Title Page

Abstract

Introduction

Conclusions

References

Tables

Figures

◀

▶

◀

▶

Back

Close

Full Screen / Esc

Printer-friendly Version

Interactive Discussion



Robbins, C. C. and Cortinas, J. V.: Local and synoptic environments associated with freezing rain in the Contiguous United States, *Weather Forecast.*, 17, 47–65, 2002.

Seidel, D. J., Ao, C. O., and Li, K.: Estimating climatological planetary boundary layer heights from radiosonde observations: comparison of methods and uncertainty analysis, *J. Geophys. Res.*, 115, D16113, doi:10.1029/2009JD013680, 2010.

Serreze, M. C., Kahl, J. D., Schnell, R. C.: Low-level temperature inversions of the Eurasian Arctic and comparisons with Soviet drifting station data, *J. Climate*, 5, 615–629, 1992.

Shulski, M. and Wendler, G.: *The Climate of Alaska*, 216 pp., University of Alaska, Fairbanks, 2007.

Stull, R.: *An Introduction to Boundary Layer Meteorology*. Kluwer Academic Publishers, Dordrecht, the Netherlands, 666 pp., 1988.

Whiteman, C. and Zhong, S.: Downslope flows on a low-angle slope and their interactions with valley inversions, *J. Appl. Meteorol.*, 47, 2023–2038, 2008.

Zhang, Y. and Seidel, D. J.: Challenges in estimating trends in Arctic surface-based inversions from radiosonde data, *Geophys. Res. Lett.*, 38, L17806, doi:10.1029/2011GL048728, 2011.

Zhang, Y., Seidel, D. J., Golaz, J.-Ch., Deser, C., and Tomas, R.: Climatological characteristics of Arctic and Antarctic surface-based inversions, *J. Climate*, 24, 5167–5186, 2011.

Methodology for determining multilayered temperature inversions

G. J. Fochesatto

Table 1. Proposed thermal layers in a temperature profile.

Layer	1	2	3	4	5	Units
T_t, z_t	-20, 100	-15, 250	-22, 550	-17, 670	-23, 1000	(°C, m)
T_b, z_b	-30, 0	-20, 100	-15, -22	-22, 550	-17, 670	(°C, m)
dT/dz	10	3.3	-2.3	4.2	-1.8	(°C/100 m)
Class	strat	strat	SBI	cold layer	EI	

Title Page

Abstract

Introduction

Conclusions

References

Tables

Figures

◀

▶

◀

▶

Back

Close

Full Screen / Esc

Printer-friendly Version

Interactive Discussion

Methodology for determining multilayered temperature inversions

G. J. Fochesatto

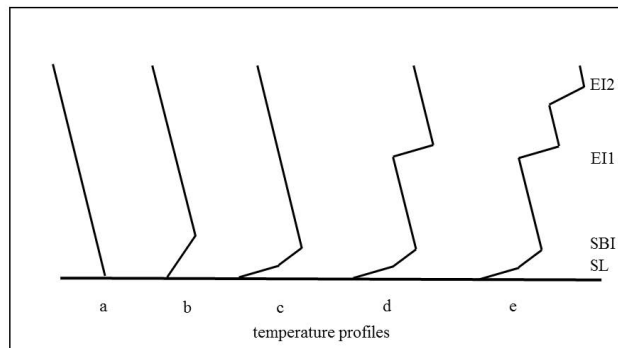


Figure 1. Illustration of temperature profiles indicating different thermodynamics conditions (a) no-inversion present; (b) presence of a SBI; (c) presence of a stratified (SL) SBI; (d) SBI stratified in the presence of an EI and (e) SBI stratified and multiple EIs. Modified after Khal (1990).

Title Page

Abstract

Introduction

Conclusions

References

Tables

Figures

◀

▶

◀

▶

Back

Close

Full Screen / Esc

Printer-friendly Version

Interactive Discussion

Methodology for determining multilayered temperature inversions

G. J. Fochesatto

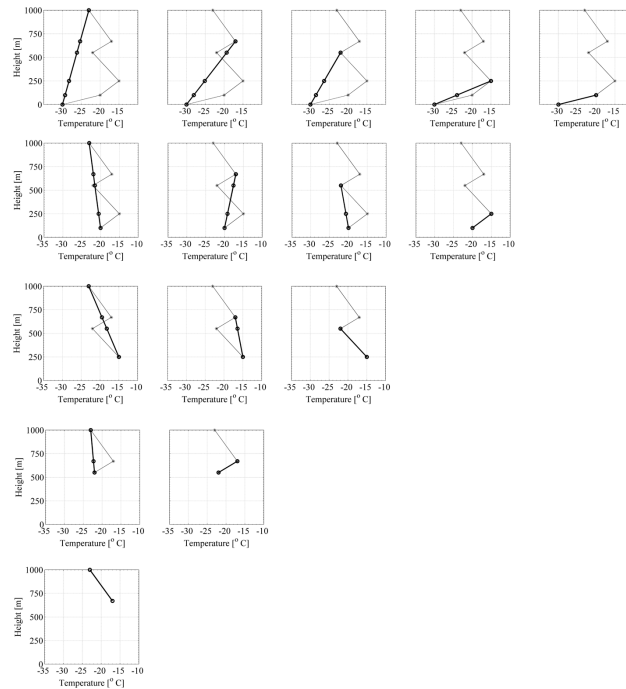


Figure 2. Sequence of the numerical routine to identify the thermal layers indicated in Table 1. Fitting function is given by the thick trace with (“o”) markers while the temperature profile is indicated by thin black trace with (“*”) markers. Top panel indicate the sequence to detect Layer 1, second panel from top is sequence to detect Layer 2, third panel from top is the detection of Layer 3, fourth panel from top is to detect Layer 4 and bottom panel is the sequence to determine Layer 5.

Title Page

Abstract

Introduction

Conclusions

References

Tables

Figures

◀

▶

◀

▶

Back

Close

Full Screen / Esc

Printer-friendly Version

Interactive Discussion

Methodology for determining multilayered temperature inversions

G. J. Fochesatto

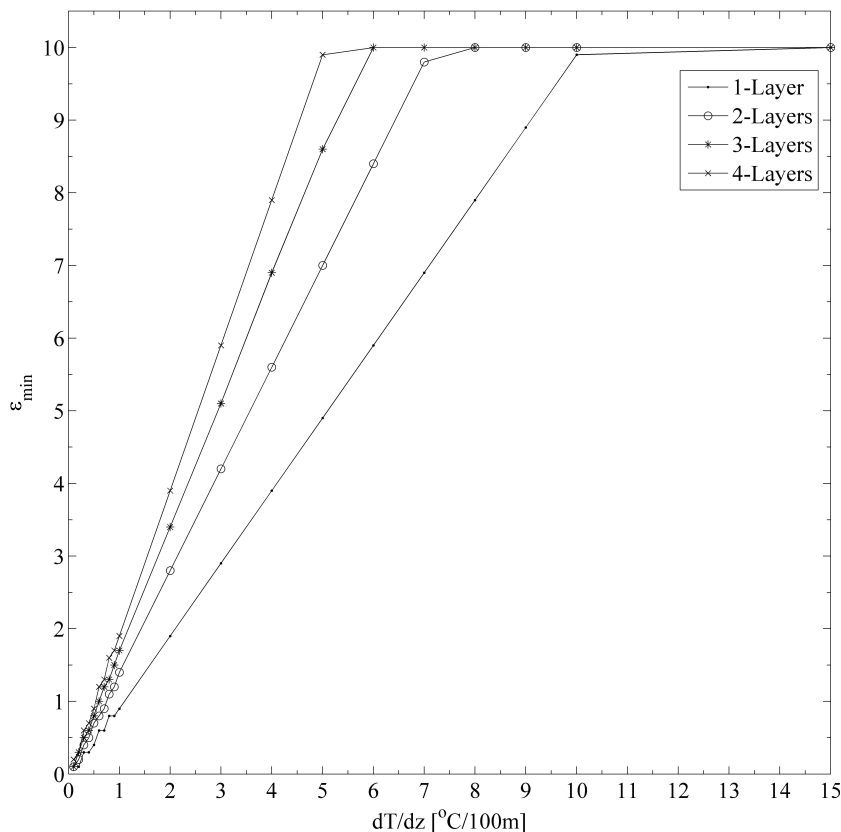


Figure 3. Preset error ϵ as function of the thermal gradient expressed in °C/100 m for detection of single thermal layer (“.”), two-layers (“o”), three-layers (“*”) and four-layers (“x”). The curves were obtained considering dT/dz from 0.1 in step of 0.1 to 1 then from 1 to 10 in steps of 1 while the error was set to a vector array from 0.1 in step of 0.1 to 10.

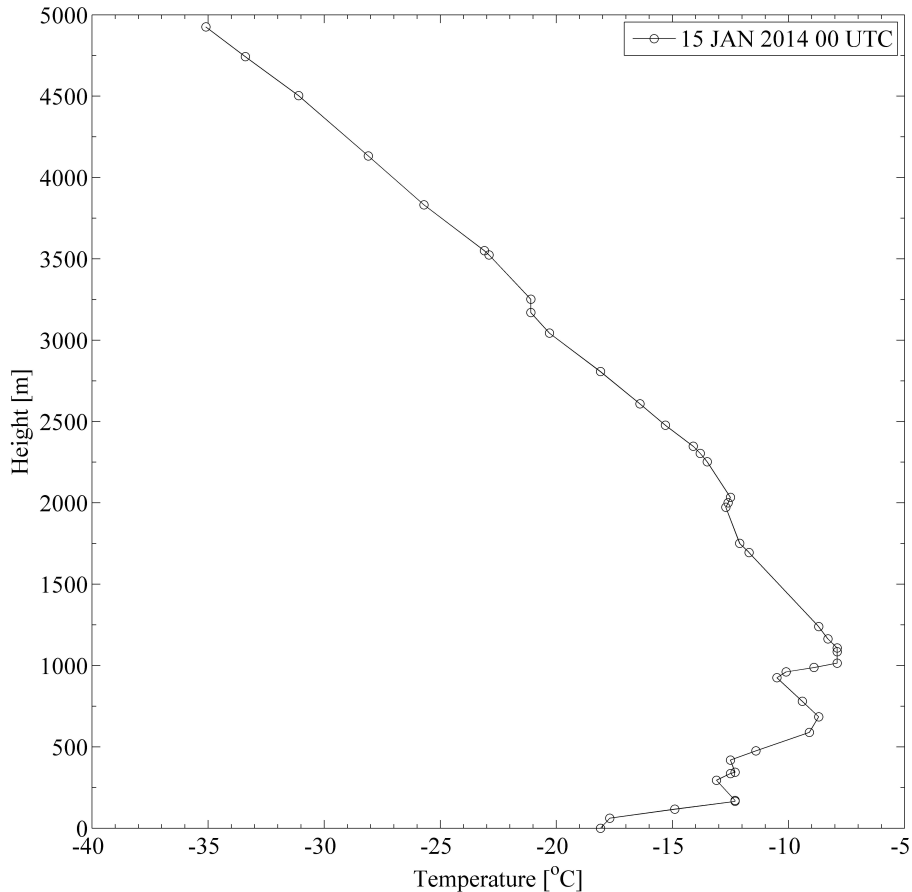


Figure 4. Radiosonde temperature profile. Observation made in 15 January 2014 at 00:00 UTC in the NWS Fairbanks International Station (code 70261). The profile display multiple inversion layers. Vertical axis id height (m) AGL at PAFA.

10581

AMTD

7, 10559–10583, 2014

Methodology for determining multilayered temperature inversions

G. J. Fochesatto

Title Page

Abstract

Introduction

Conclusions

References

Tables

Figures

◀

▶

◀

▶

Back

Close

Full Screen / Esc

Printer-friendly Version

Interactive Discussion



Methodology for determining multilayered temperature inversions

G. J. Fochesatto

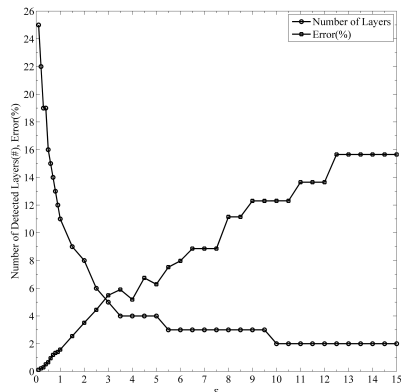


Figure 5. Retrieved number of thermal layers (“o”) and final temperature profile error (“□”) as function of the ϵ convergence preset value.

[Title Page](#)
[Abstract](#)
[Introduction](#)
[Conclusions](#)
[References](#)
[Tables](#)
[Figures](#)
[◀](#)
[▶](#)
[◀](#)
[▶](#)
[Back](#)
[Close](#)
[Full Screen / Esc](#)
[Printer-friendly Version](#)
[Interactive Discussion](#)


Methodology for determining multilayered temperature inversions

G. J. Fochesatto

Title Page

Abstract

Introduction

Conclusions

References

Tables

Figures

◀

▶

◀

▶

Back

Close

Full Screen / Esc

Printer-friendly Version

Interactive Discussion

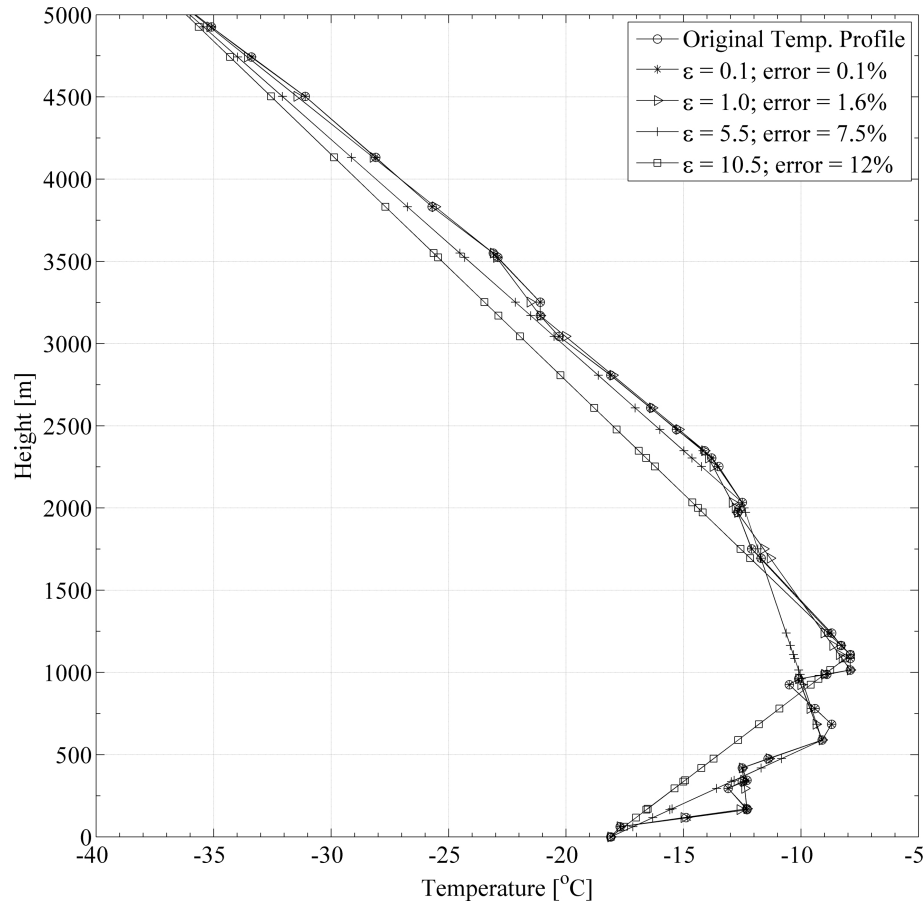


Figure 6. Resampled temperature profile after running the numerical methodology over different preset convergence error values $\epsilon = 0.1, 1.0, 5.5, 10.5$ as function of the final retrieved error profile in (%).